Journal of Geophysical Research: Oceans

Supporting Information for

ENSO Phase Transitions in a Warming Climate: Multi-Model Large Ensemble Analysis

Brandon A. Molina[1], Sara C. Sanchez[1], Clara Deser[2], Nicola Maher[3,4], and Pedro DiNezio[1,5]

[1]Department of Atmospheric and Oceanic Sciences, University of Colorado, Boulder, CO, USA, [2]National Center for Atmospheric Research, Boulder, CO, USA, [3]Research School of Earth Sciences, Australian National University, Canberra, Australia, [4]ARC Centre of Excellence for 21st Century Weather, Australia, [5]ATLAS Institute University of Colorado, Boulder, CO, USA

Contents of this file

Figures S1 to S12

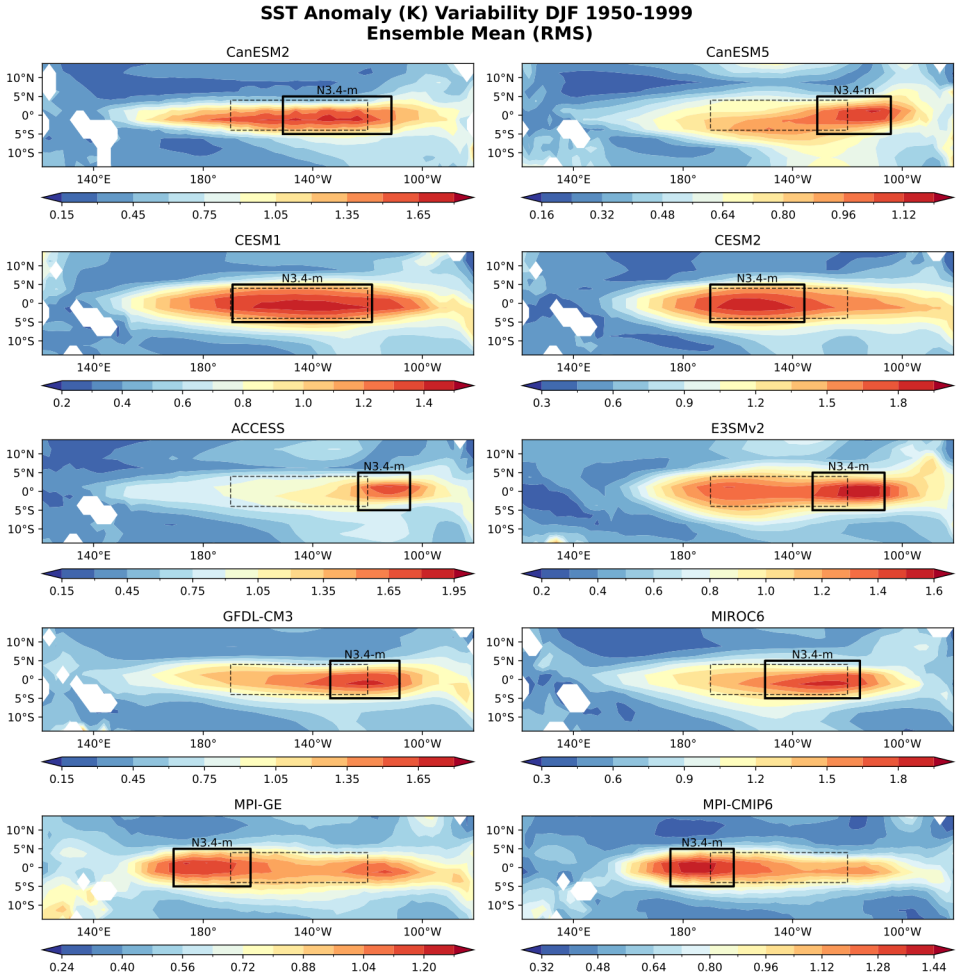

Figure S1: Multi-Model Representation of Tropical Pacific SST Anomaly Variability during DJF (1950–1999). Individual panels display the ensemble mean Root Mean Square (RMS) of the standard deviation (S.D.) of Sea Surface Temperature (SST) anomalies (K) for ten climate models over the 1950–1999 period. In each panel, the dashed rectangle identifies the standard Niño-3.4 region (5°S–5°N, 170°W–120°W). The solid black rectangle denotes the modified Niño-3.4 region (N3.4-m), designed to dynamically account for spatial biases in each model's historical representation of ENSO. To determine the N3.4-m boundaries, the member-averaged RMS of SST anomalies are first meridionally averaged between 5°S and 5°N to identify the longitude of peak variability. The western and eastern boundaries are then established at the longitudes where the zonal mean drops below 93% of the peak value. CESM1 was selected as the baseline for this specific calibration threshold to approximate the standard Niño-3.4 width. This choice is supported by multi-model evaluations (e.g., Planton et al., 2021) showing that CESM1 exhibits high fidelity in its spatial representation of ENSO and outperforms the broader CMIP ensemble mean.

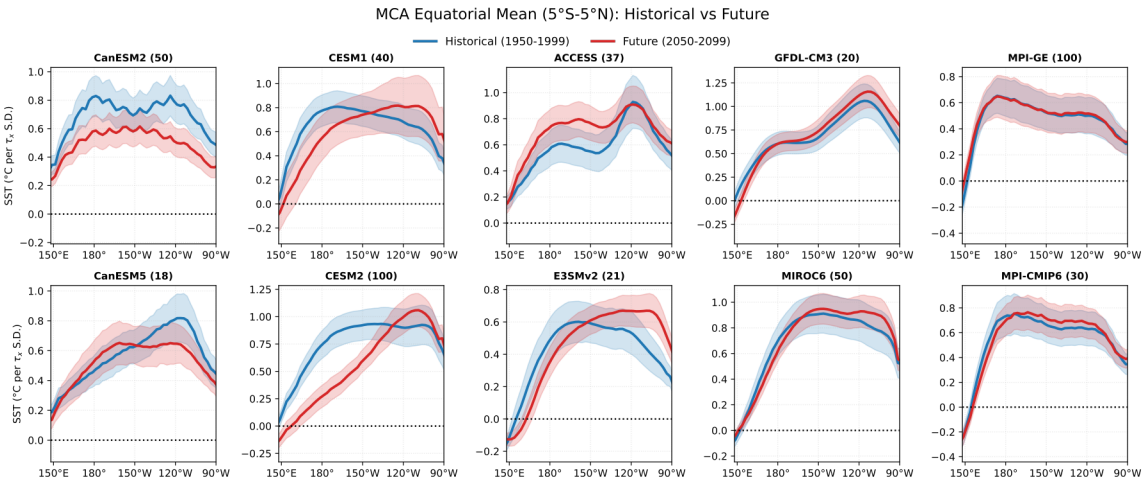

Figure S2: Historical vs. 21st-century equatorial SST heterogeneous patterns during MAM. Longitudinal profiles depict meridional averages across the equatorial Pacific for ten climate models. Solid lines indicate the ensemble mean for the historical (1950–1999; blue) and projected future (2050–2099; red) periods. Shading denotes ±1 S.D. of the ensemble spread.

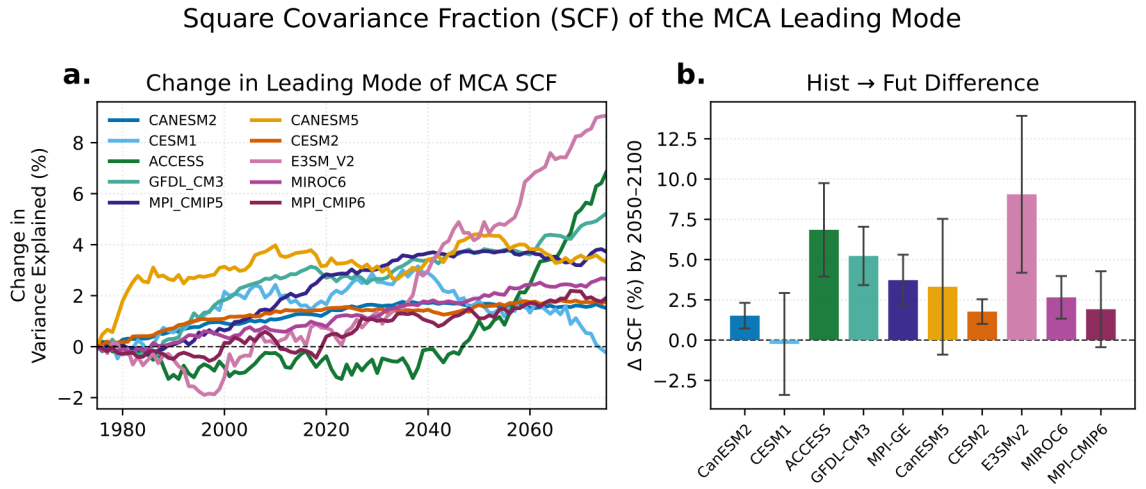

Figure S3: Temporal Evolution and Projected Changes in the Leading Mode of the Squared Covariance Fraction (SCF). (a) The temporal trajectory of the change in variance explained (%) by the leading MCA mode relative to the historical baseline. The x-axis represents the center year of 50-year periods for each of the 10 climate models, spanning from 1975 to 2075. (b) The projected change in SCF (ΔSCF) by the 2050–2099 period compared to the historical reference. Bars denote the ensemble mean change for each model, and error bars represent the 95% confidence interval of the ensemble-mean change (two-tailed Student's t-test).

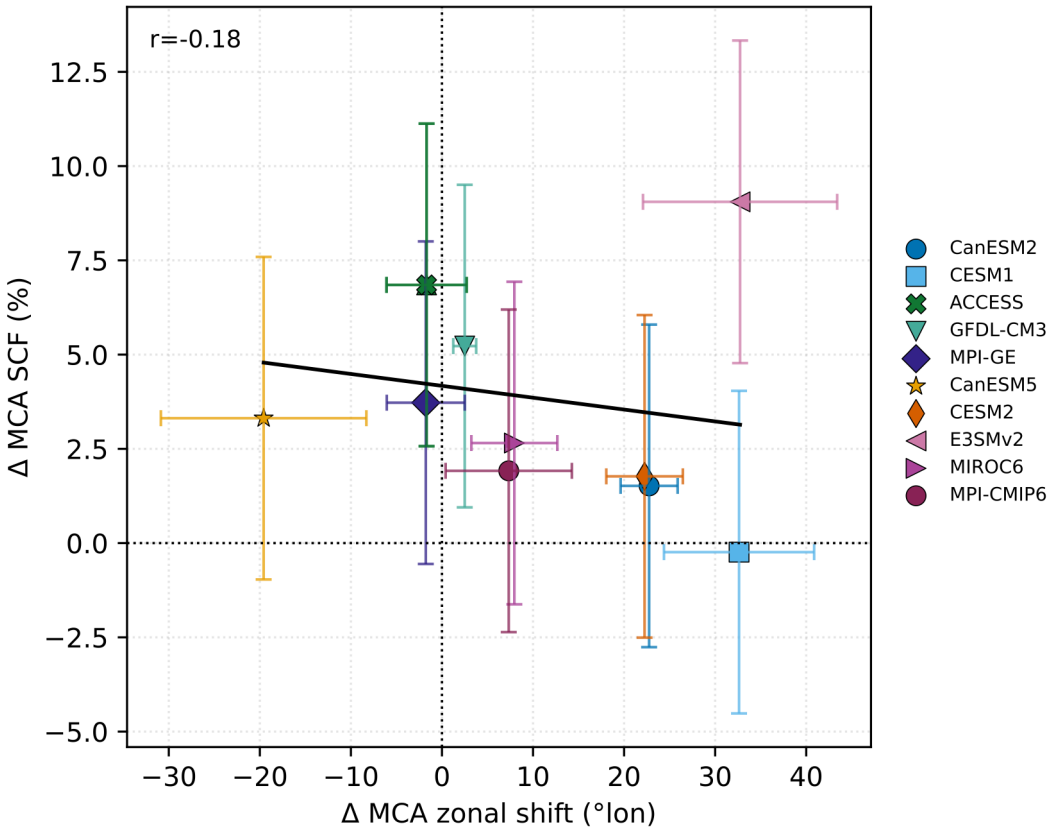

Figure S4: Relationship Between Changes in Air-Sea Coupling Strength (SCF) and Zonal Coupling Shifts. The x-axis denotes the forced zonal shift in the center of action (°lon; derived from the MCA patterns in Figure 3), where positive values indicate an eastward shift toward the eastern Pacific. The y-axis shows the corresponding change in the Squared Covariance Fraction (expressed as a percentage; derived from the MCA patterns in Figure S3) between the historical (1950–1999) and projected future (2050–2099) periods, where positive values indicate an intensification in the strength of the dominant seasonal coupling mode. Each marker represents the ensemble mean for one of the 10 climate models, with colors and shapes as indicated in the legend. Horizontal and vertical error bars denote the 95% confidence interval of the inter-ensemble spread. The solid black line represents the inter-model linear regression, with the Pearson correlation coefficient (r) indicated in the upper-left corner.

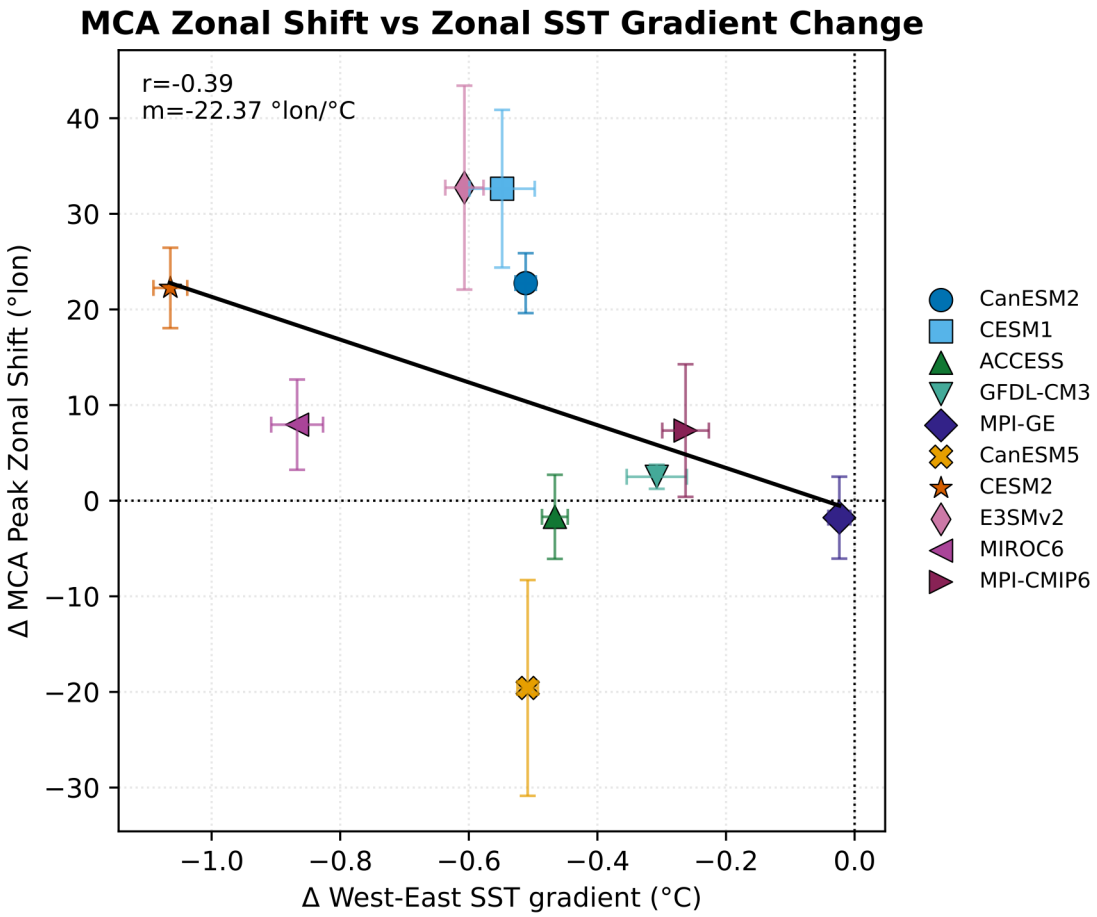

Figure S5: Inter-model Relationship Between Equatorial SST Gradient Changes and Zonal Shifts in Air-Sea Coupling. The scatter plot illustrates the relationship between the projected change in the west-east equatorial SST gradient (x-axis) and the shift in the MCA peak zonal location (y-axis). Each marker represents the ensemble mean for one of the 10 climate models, with colors and shapes as indicated in the legend. Horizontal and vertical error bars denote the 95% confidence interval of the ensemble-mean change (two-tailed Student's t-test). The solid black line represents the inter-model linear regression, with the Pearson correlation coefficient (r) and the regression slope indicated in the upper-left corner. Horizontal and vertical dotted lines signify the zero-change baseline relative to the historical reference period (1950–1999).

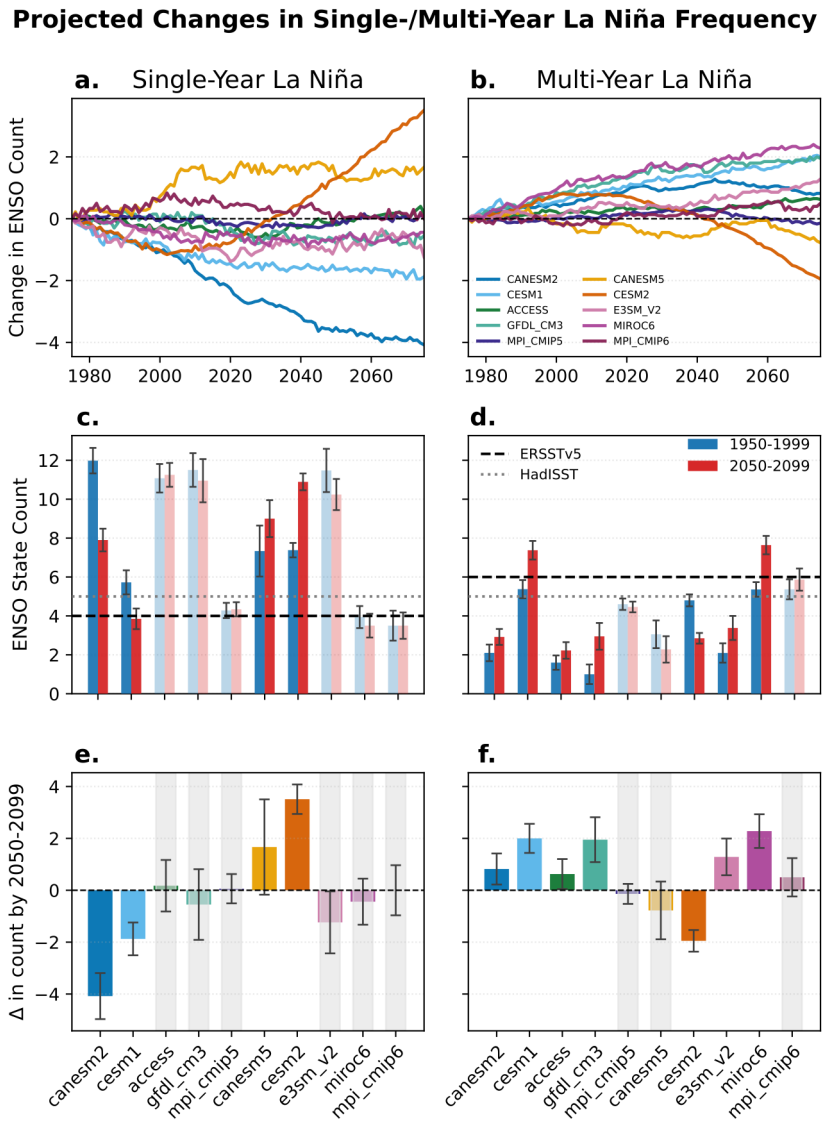

Figure S6: Projected Changes in Single- and Multi-Year La Niña Frequency. (a)–(b) Temporal trajectories of the change in event count for (a) single-year and (b) multi-year La Niña events relative to the historical baseline (1950–1999). The x-axis indicates the center year of a 50-year sliding window, spanning from 1975 to 2075. (c)–(d) Total event counts for the historical (1950–1999; blue) and projected future (2050–2099; red) periods across the 10-model ensemble. Horizontal dashed and dotted lines represent observational benchmarks from ERSSTv5 and HadISST, respectively. Greyed out bars in panels (c) and (d) signify models where the difference between historical and future event counts is not statistically significant. (e)–(f) Projected shift (Δ in count) by the 2050–2099 period. Error bars represent the 95% confidence interval of the ensemble-mean change (two-tailed Student's t-test), and vertical grey shading in panels (e) and (f) identifies models where the projected change in frequency is not statistically significant ($p > 0.05$) according to a two-tailed Welch's t-test.

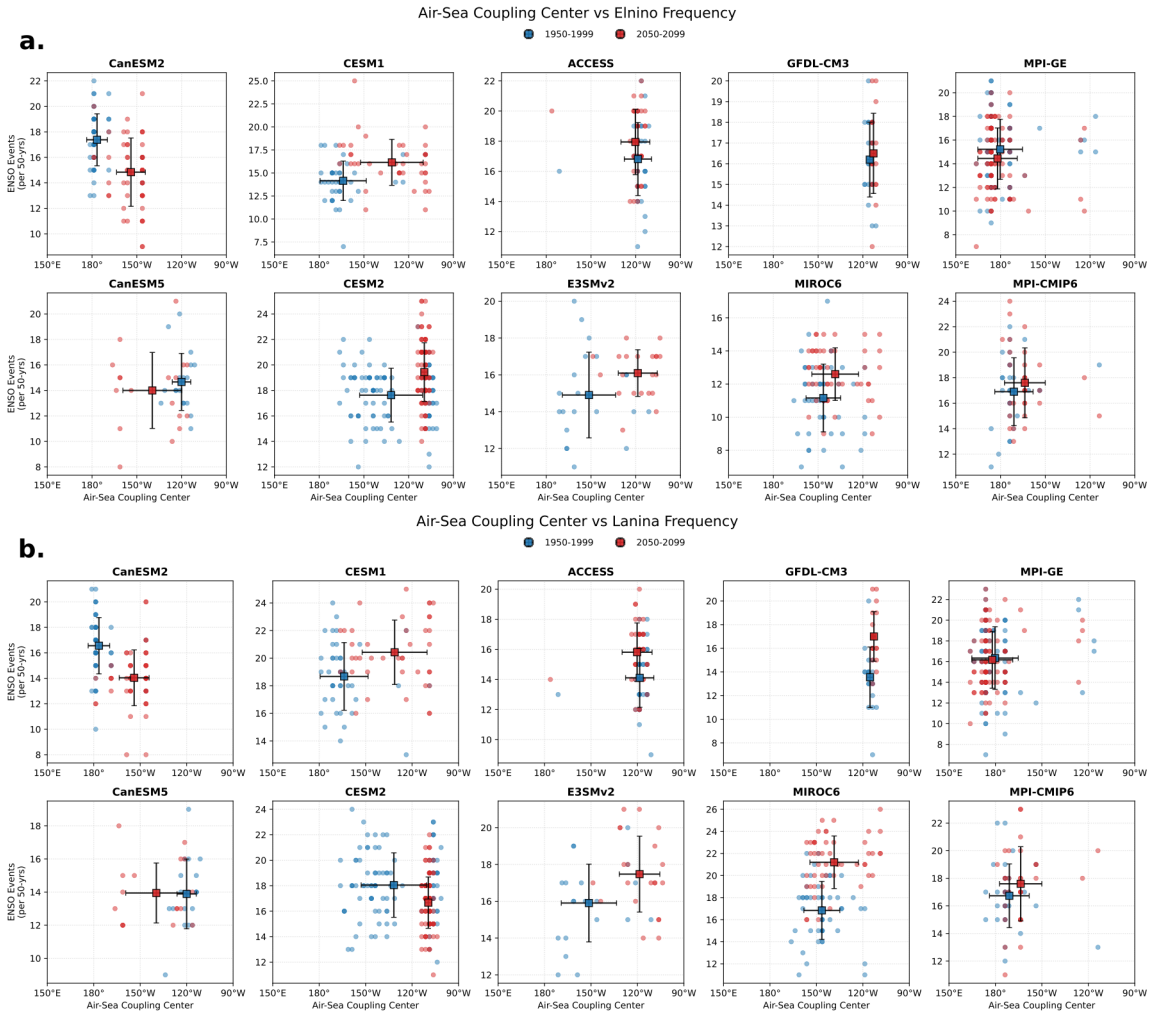

Figure S7: Relationship Between Intra-Ensemble Zonal Coupling Shifts and ENSO Phase-Frequency Changes. Scatter plots illustrate the relationship between the longitude of the air-sea coupling center (x-axis) and the event frequency (events per 50 years; y-axis) across the 10 climate models for (a) El Niño and (b) La Niña states. Small, semi-transparent circular markers represent individual ensemble members, with colors distinguishing the historical reference period (1950–1999; blue) from the late 21st century (2050–2099; red). Larger, black-outlined circular markers denote the multi-member ensemble mean for each model, and the horizontal and vertical whiskers represent the corresponding standard deviation (σ) spread of the ensemble members.

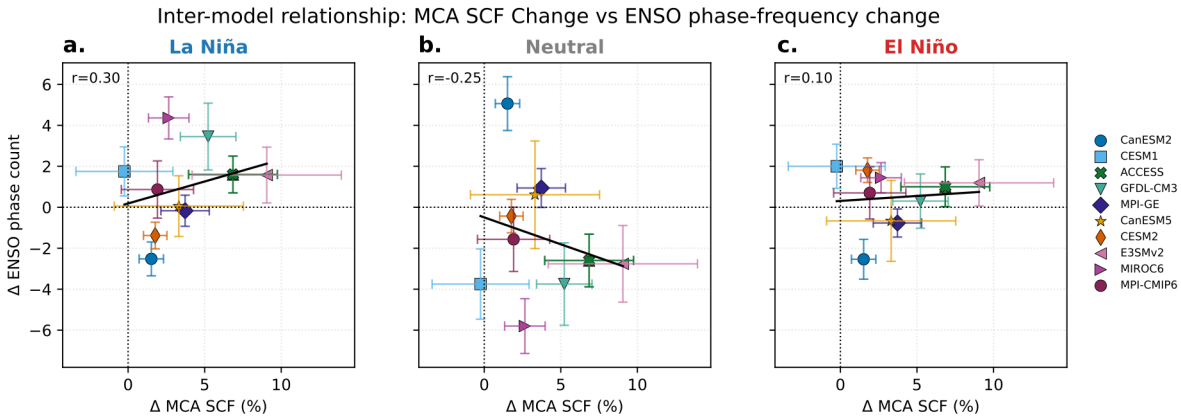

Figure S8: Relationship Between Changes in Air-Sea Coupling Strength (SCF) and ENSO Phase-Frequency. The x-axis denotes the change in the Squared Covariance Fraction (%; derived from the MCA patterns in Figure S3) between the historical (1950–1999) and projected future (2050–2099) periods, where positive values indicate an intensification in the strength of the dominant seasonal coupling mode. The y-axis shows the corresponding change in the ENSO phase count for (a) La Niña, (b) Neutral, and (c) El Niño states. Each marker represents the ensemble mean for one of the 10 climate models, with colors and shapes as indicated in the legend. Horizontal and vertical error bars denote the 95% confidence interval of the inter-ensemble spread. The solid black line in each panel represents the inter-model linear regression, with the Pearson correlation coefficient (r) indicated in the upper-left corner.

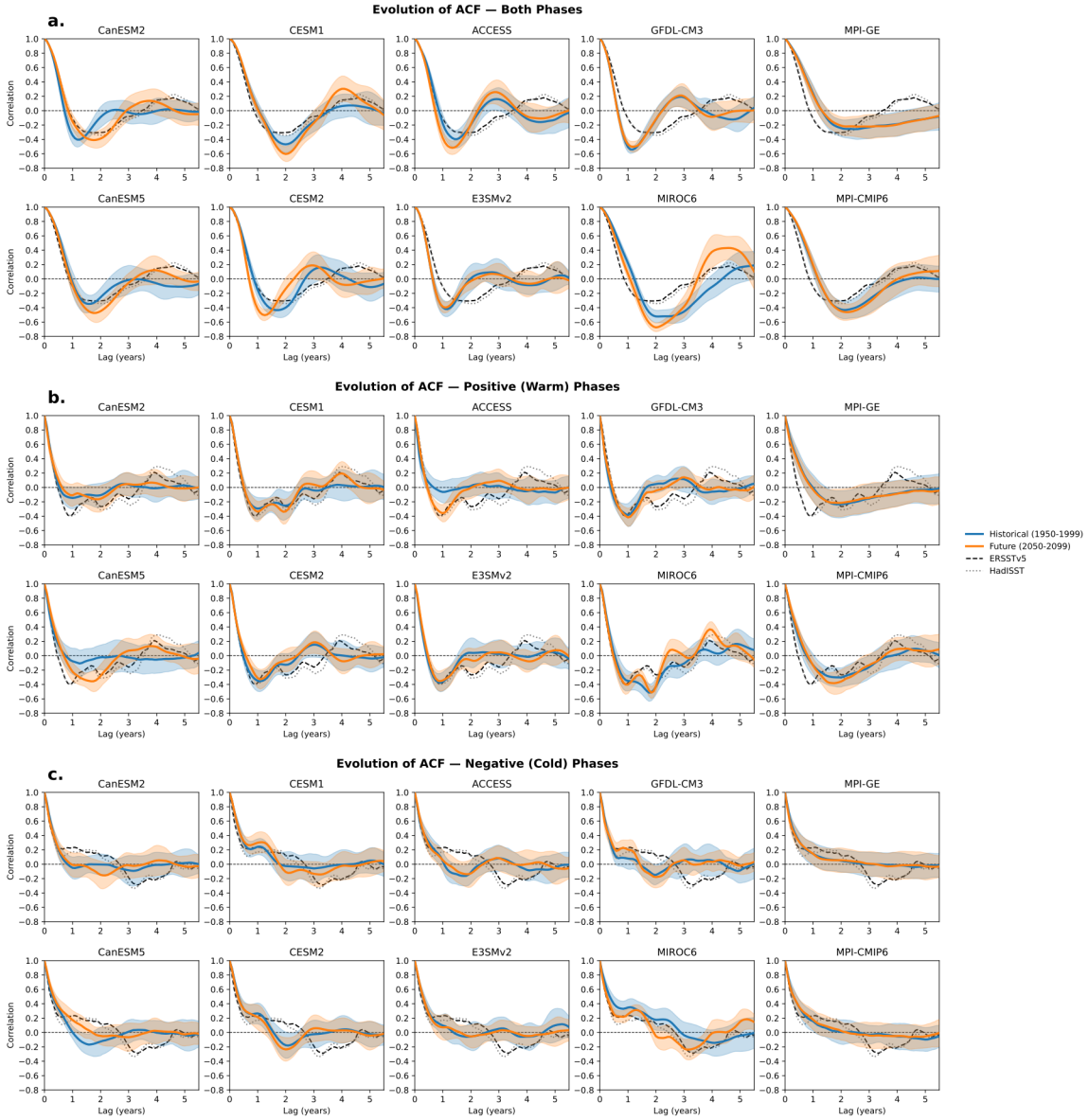

Figure S9. Multi-model comparison of historical (1950–1999) and late 21st century (2050–2099) Niño 3.4 autocorrelation functions (ACF). (a) Full Phase ACF computed from the modified Niño3.4 (N3.4-m) time series. (b) Positive (Warm) Phase ACF, isolating months where anomalies exceed +0.5 S.D. of each dataset's 1950–1999 climatological distribution. (c) Negative (Cold) Phase ACF, isolating months where anomalies exceed −0.5 S.D. Each panel shows ACF as a function of lag (0–5 years) for one of the 10 climate models. Blue solid lines indicate the ensemble-mean historical ACF (1950–1999); orange solid lines indicate the ensemble-mean future ACF (2050–2099). Shading denotes ±1 S.D. of the ensemble spread. Black dashed and grey dotted lines show observational benchmarks from ERSSTv5 and HadISST over 1950–1999, respectively.

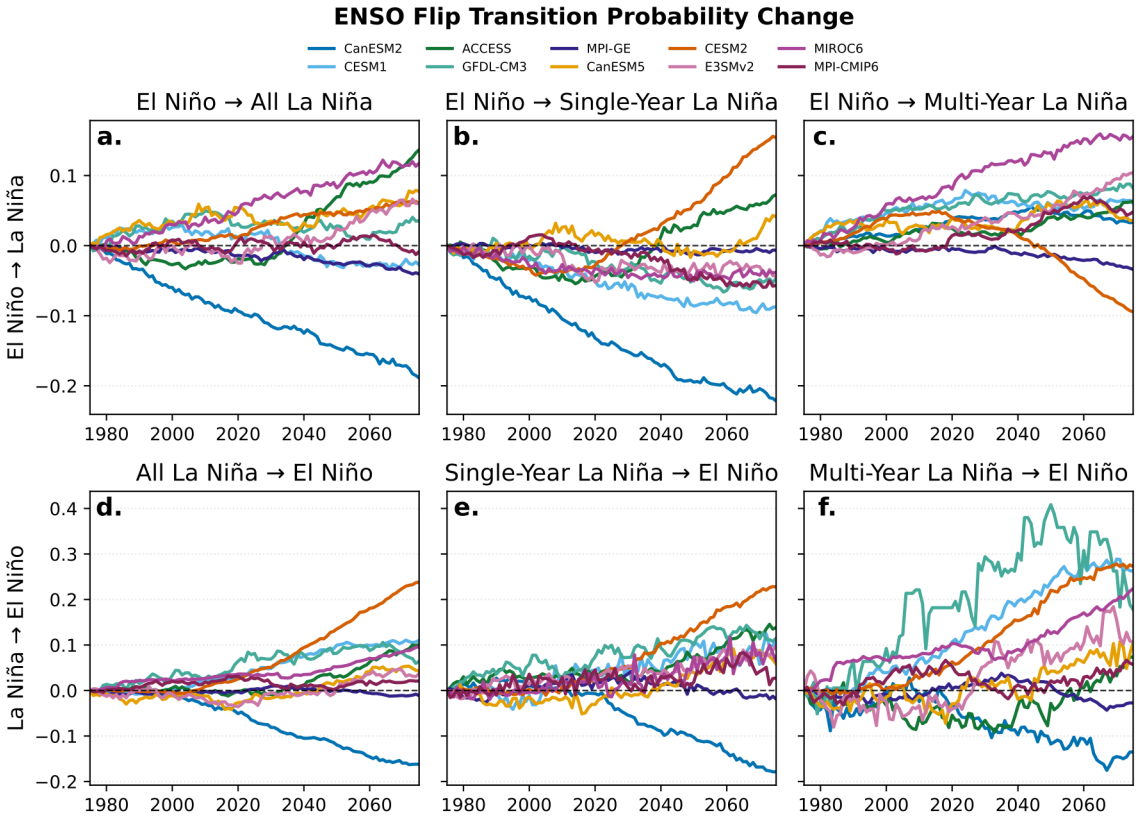

Figure S10: Temporal Evolution of Projected Changes in ENSO Flip Transition Probabilities. Trajectories illustrate the change in transition probability relative to the historical reference period (1950–1999) across a 50-year sliding window, with the x-axis indicating the window's center year. (a)–(c) The top row depicts transitions initiated from El Niño into (a) all, (b) single-year, and (c) multi-year La Niña durations. (d)–(f) The bottom row displays the reverse transitions from (d) all, (e) single-year, and (f) multi-year La Niña durations back into El Niño. Individual colored lines represent the ensemble mean for each of the 10 climate models, and the horizontal dashed line in each panel indicates the zero-change baseline.

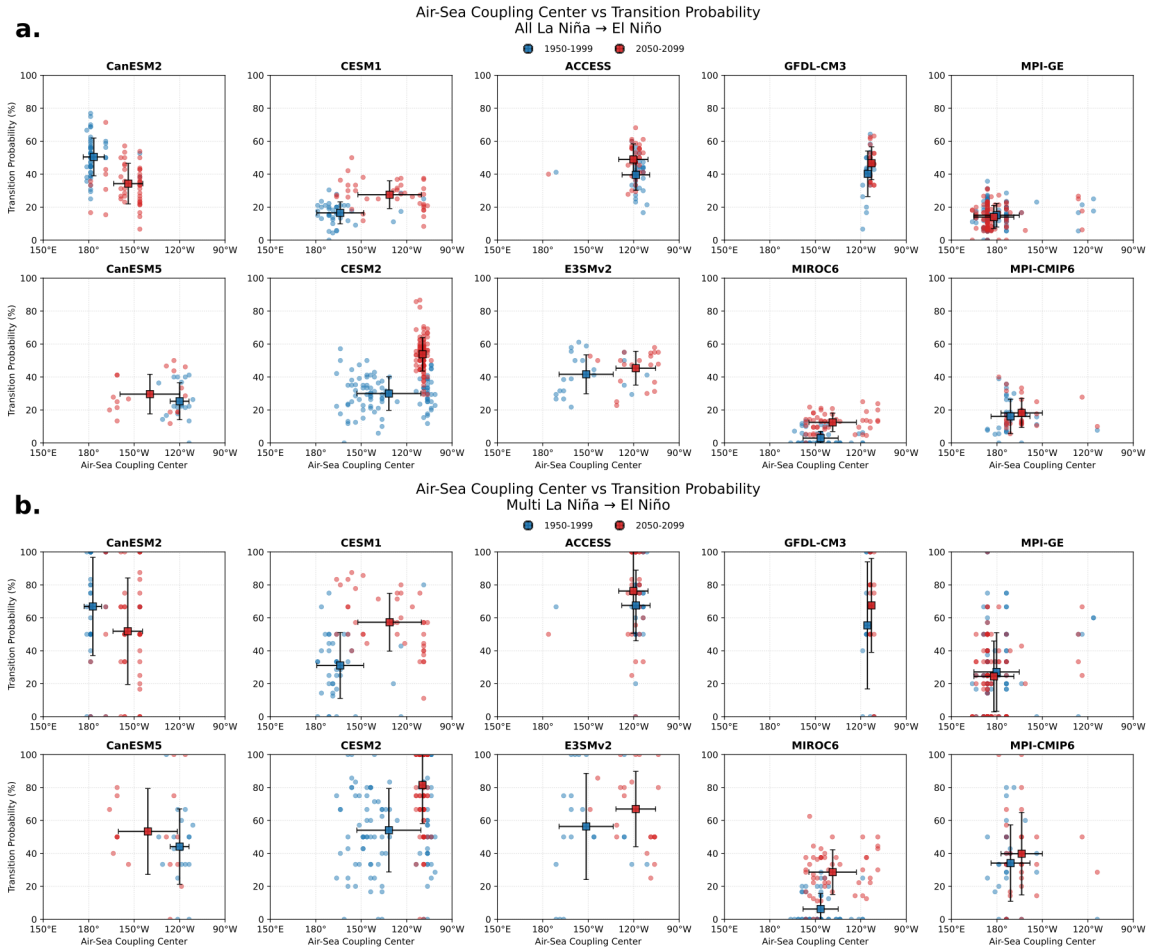

Figure S11: Inter-member Relationship Between Coupling Longitudes and ENSO Transition Probabilities. Scatter plots illustrate the relationship between the longitude of the air-sea coupling center (x-axis) and the phase-transition probability (%; y-axis) across the 10 climate models for (a) All La Niña to El Niño transitions and (b) Multi-Year La Niña to El Niño transitions. Small, semi-transparent circular markers represent individual ensemble members, with colors distinguishing the historical reference period (1950–1999; blue) from the late 21st century (2050–2099; red). Larger, black-outlined circular markers denote the multi-member ensemble mean for each model, and the horizontal and vertical whiskers represent the corresponding standard deviation (σ) spread of the ensemble members.

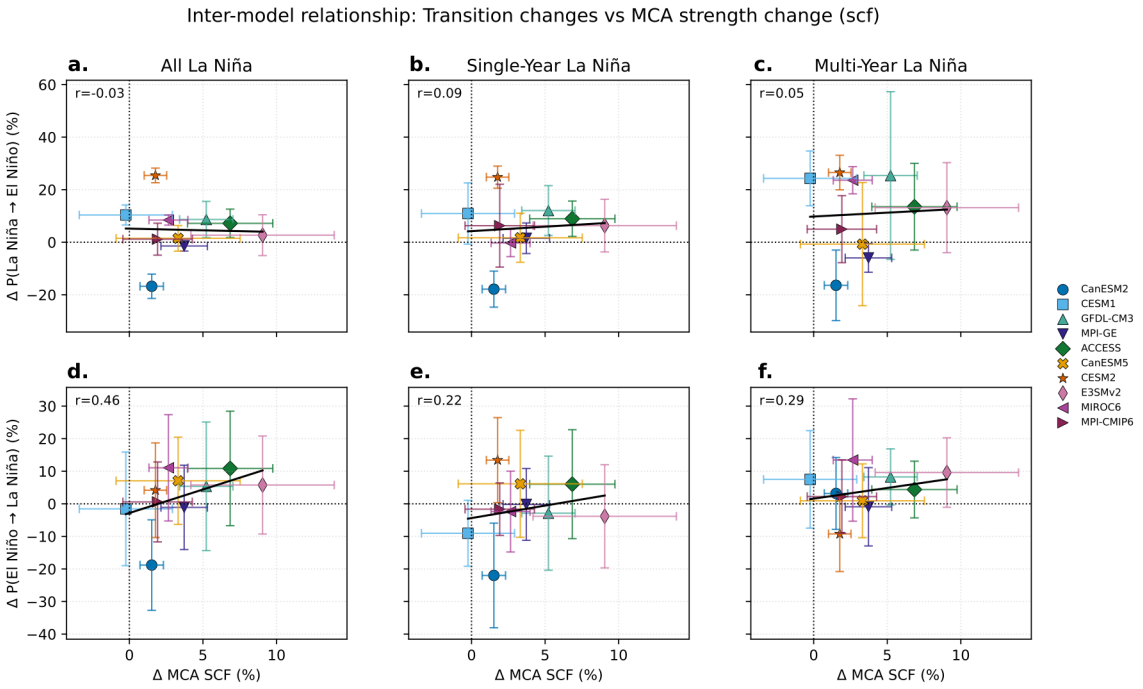

Figure S12: Relationship Between Changes in Air-Sea Coupling Strength (SCF) and ENSO Phase Transition Probabilities. The x-axis denotes the change in the Squared Covariance Fraction (%; derived from the MCA patterns in Figure S3) between the historical (1950–1999) and projected future (2050–2099) periods, where positive values indicate an intensification in the strength of the dominant seasonal coupling mode. The y-axis shows the corresponding change in transition probability (ΔP; %) between the historical and future periods. (a)–(c) The top row illustrates the relationship for transitions from La Niña to El Niño, categorized by (a) All La Niña, (b) Single-Year La Niña, and (c) Multi-Year La Niña initial states. (d)–(f) The bottom row tracks the reverse transitions from El Niño into (d) All La Niña, (e) Single-Year La Niña, and (f) Multi-Year La Niña resulting durations. Each marker represents the ensemble mean for one of the 10 climate models, with colors and shapes as indicated in the legend. Horizontal and vertical error bars denote the 95% confidence interval of the inter-ensemble spread. The solid black line in each panel represents the inter-model linear regression, with the Pearson correlation coefficient (r) indicated in the upper-left corner.